

Alterations in Left Ventricular Torsion and Diastolic Recoil After Myocardial Infarction With and Without Chronic Ischemic Mitral Regurgitation

Frederick A. Tibayan, MD; Filiberto Rodriguez, MD; Frank Langer, MD; Mary K. Zasio, BS; Lynn Bailey, AS; David Liang, MD, PhD; George T. Daughters, MS; Neil B. Ingels, Jr, PhD; D. Craig Miller, MD

Background—Chronic ischemic mitral regurgitation (CIMR) is associated with heart failure that continues unabated whether the valve is repaired, replaced, or ignored. Altered left ventricular (LV) torsion dynamics, with deleterious effects on transmural gradients of oxygen consumption and diastolic filling, may play a role in the cycle of the failing myocardium. We hypothesized that LV dilatation and perturbations in torsion would be greater in animals in which CIMR developed after inferior myocardial infarction (MI) than in those that it did not.

Methods— 8 ± 2 days after marker placement in sheep, 3-dimensional fluoroscopic marker data (baseline) were obtained before creating inferior MI by snare occlusion. After 7 ± 1 weeks, the animals were restudied (chronic). Inferior MI resulted in CIMR in 11 animals but not in 9 (non-CIMR). End-diastolic septal-lateral and anterior-posterior LV diameters, maximal torsional deformation (ϕ_{\max} , rotation of the LV apex with respect to the base), and torsional recoil in early diastole ($\phi_{5\%}$, first 5% of filling) for each LV free wall region (anterior, lateral, posterior) were measured.

Results—Both CIMR and non-CIMR animals demonstrated derangement of LV torsion after inferior MI. In contrast to non-CIMR, CIMR animals exhibited greater LV dilation and significant reductions in posterior maximal torsion ($6.1\pm 4.3^\circ$ to $3.9\pm 1.9^\circ$ * versus $4.4\pm 2.5^\circ$ to $2.8\pm 2.0^\circ$; mean \pm SD, baseline to chronic, * $P<0.05$) and anterior torsional recoil ($-1.4\pm 1.1^\circ$ to $-0.2\pm 1.0^\circ$ versus $-1.2\pm 1.0^\circ$ to $-1.3\pm 1.6^\circ$).

Conclusion—MI associated with CIMR resulted in greater perturbations in torsion and recoil than inferior MI without CIMR. These perturbations may be linked to more LV dilation in CIMR, which possibly reduced the effectiveness of fiber shortening on torsion generation. Altered torsion and recoil may contribute to the “ventricular disease” component of CIMR, with increased gradients of myocardial oxygen consumption and impaired diastolic filling. These abnormalities in regional torsion and recoil may, in part, underlie the “ventricular disease” of CIMR, which may persist despite restoration of mitral competence. (*Circulation*. 2004;110[suppl II]:II-109–II-114.)

Key Words: myocardial infarction ■ mitral valve ■ mechanics

Chronic ischemic mitral regurgitation (CIMR) is an important complication after myocardial infarction (MI) and is linked to increased mortality that is independent of the degree of underlying left ventricular (LV) dysfunction.¹ Repairing or replacing the valve fails to change the mortality curve dramatically, suggesting that the primary problem lies in the myocardium.² Supporting this idea, changes in LV geometry, such as LV dilation, are powerful predictors of adverse outcome.³ In dilated cardiomyopathy⁴ and chronic mitral regurgitation (MR),⁵ such geometric remodeling (ie, increased LV volume [LVV] or LV

diameter) has been linked to decreases in LV systolic torsion and early diastolic recoil, which, in turn, likely contribute to a cycle of progressive LV functional decline.

We surmised that derangement in torsion might play a role in the “ventricular disease” element of CIMR. Therefore, we tested the hypotheses that inferior MI is associated with alterations in torsion and recoil, and that these postinfarct alterations would be greater in animals in which CIMR developed than in those in which CIMR did not develop.

From Department of Cardiovascular and Thoracic Surgery (F.A.T., F.R., F.L., M.K.Z., G.T.D., N.B.I., D.C.M.), Division of Cardiovascular Medicine and Stanford University School of Medicine (L.B., D.L.), Stanford, Calif; Laboratory of Cardiovascular Physiology and Biophysics; Research Institute of the Palo Alto Medical Foundation (G.T.D., N.B.I.), Palo Alto, Calif.

Correspondence to D. Craig Miller, MD, Department of Cardiovascular and Thoracic Surgery, Falk Cardiovascular Research Center, Stanford University School of Medicine, Stanford, CA 94305-5247. E-mail dcm@stanford.edu

Supported by grants HL-29589 and HL-67025 from the National Heart, Lung, and Blood Institute (NHLBI). Drs. Tibayan, Rodriguez, and Langer are Carl and Leah McConnell Cardiovascular Surgical Research Fellows. Dr. Tibayan was supported by NHLBI Individual Research Service Award HL-67563. Dr. Rodriguez was supported by grant HL67025-01-S1 from the NHLBI and was a recipient of an American College of Surgeons Resident Research Scholarship Award. Dr. Langer was also supported by the Department of Thoracic and Cardiovascular Surgery, University Hospitals Homburg, Homburg/Saar, Germany.

© 2004 American Heart Association, Inc.

Circulation is available at <http://www.circulationaha.org>

DOI: 10.1161/01.CIR.0000138385.05471.41

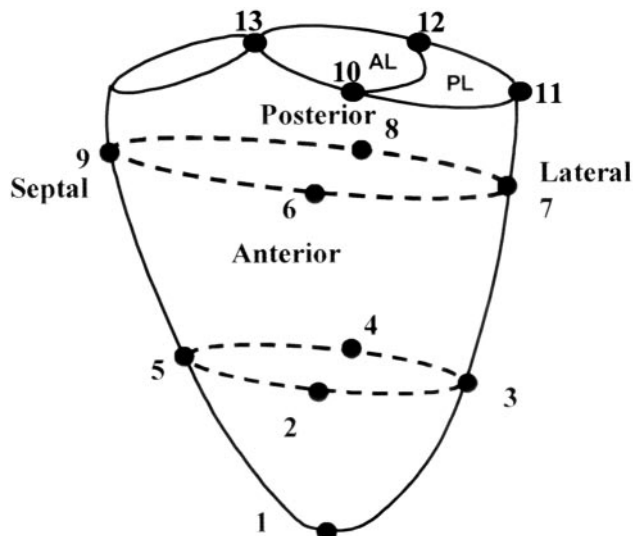


Figure 1. Schematic of marker array used in this study. The aortic valve is shown for reference. One marker (1) is placed at the apex, with markers placed around 4 meridians (anterior, lateral, posterior, septal) at 2 levels, apical (2 to 5) and basal (6 to 9).

Methods

Surgical Preparation

Forty Dorsett hybrid sheep (71±5 kg; R.E. McGrew Livestock, Dixon, Calif) were premedicated with ketamine (25 mg/kg intramuscular), and anesthesia was induced with sodium thiopental (6.8 mg/kg intravenous) and maintained with inhalation isoflurane (1 to 2.5%). Through a left thoracotomy, 8 tantalum myocardial markers (2 to 9; Figure 1) were inserted in the LV epicardial layer along 4 equally spaced longitudinal meridians, with 1 marker (1) at the LV apex. Polypropylene 2-0 sutures were passed loosely around the 1, 2, or, occasionally, 3 obtuse marginal branches of the left circumflex coronary artery located between the posterior vein of the left ventricle and the middle cardiac vein, and loosely snared using the method of Llaneras et al.⁶ On cardiopulmonary bypass, tantalum markers were placed on the tips of the anterior and posterior papillary muscles, around the mitral annulus, and at the edge of each mitral leaflet for use in previously published studies.⁷ Figure 1 shows the LV markers used for analysis in the present study. A micromanometer pressure transducer (PA4.5-X6; Konigsberg Instruments, Inc) was placed in the LV chamber through the apex.

Experimental Protocol

After 8±2 days, each animal was taken to the cardiac catheterization laboratory, sedated with ketamine (1 to 4 mg/kg per hour intravenous infusion) and diazepam (5-mg intravenous bolus as needed), intubated, mechanically ventilated, and maintained with inhalation isoflurane (1 to 2.5%). Transesophageal echocardiography and coronary angiography were performed and baseline videofluoroscopic marker and hemodynamic data acquired.

After premedication with lidocaine (100 mg intravenous), bretylium (75 mg intravenous), and magnesium (3 g intravenous), the coronary artery snares were tightened and complete occlusion of the selected vessels was verified by angiography. An epinephrine drip was titrated to maintain coronary perfusion pressure (aortic diastolic pressure minus LV diastolic pressure) >60 mm Hg. Ventricular arrhythmias were treated with lidocaine (50 to 100 mg intravenous) and amiodarone (50 to 150 mg intravenous), as needed. The animal was then stabilized and recovered. The animals were followed-up for clinical signs of heart failure (tachypnea, lethargy, anorexia), and serial transthoracic echocardiography was used to detect LV dilatation and MR.

After 7±1 weeks, the animals were returned to the cardiac catheterization laboratory for recording of hemodynamic, transesophageal echocardiography, and marker data. MR was graded based on regurgitant jet extent and width as none (0), trace (+0.5), mild (+1), moderate (+2), moderate-severe (+3), or severe (+4) by an experienced echocardiographer (D.L.) using a 3-chamber view (approximately equivalent to the vertical plane in a human study).

All animals received humane care in compliance with the *Principles of Laboratory Animal Care* formulated by the National Society for Medical Research and the *Guide for Care and Use of Laboratory Animals* prepared by the National Academy of Sciences and published by the National Institutes of Health (DHEW NIHG publication 85-23, revised 1985). This study was approved by the Stanford University Medical School Laboratory Research Animal Review committee and conducted according to Stanford University policy.

Data Acquisition

Images were acquired with the animal in the right lateral position with a biplane videofluoroscopy system (Philips Medical Systems, North America Company). Data from 2 radiographic views were digitized and merged to yield 3-dimensional coordinates for each of the radio-opaque markers every 16.7 ms using custom-designed software. Ascending aortic pressure, LV pressure, and electrocardiogram voltage signals were digitized and recorded simultaneously at end-expiration during marker data acquisition. Konigsberg catheters were calibrated using micromanometer pressure transducers (Millar Instruments, Inc) temporarily placed during the study.

Data Analysis

Ten animals died postoperatively, primarily of respiratory complications after cardiopulmonary bypass. Of the 30 animals that underwent coronary occlusion, 10 died acutely secondary to refractory ventricular arrhythmias. The remaining 20 animals were divided into 2 groups on the basis of severity of MR at the time of the second study: 9 did not have MR (MR <1.5; “non-CIMR” group), and 11 had chronic ischemic MR (MR ≥2; “CIMR” group).

Hemodynamics and Cardiac Cycle Timing

Three consecutive steady-state beats before infarction were averaged and defined as “baseline” data for each animal. Similarly, at the follow-up study, 3 beats were averaged and termed “chronic” data. During each cardiac cycle, end-systole was defined as the time of the videofluoroscopic frame containing the point of peak negative rate of LV pressure decrease (−dP/dt), and end-diastole was defined as the videofluoroscopic frame before the upstroke in LVP. Instantaneous LVV was calculated from the positions of the epicardial LV markers and annular markers using a space-filling multiple tetrahedral volume method for each frame, ie, every 16.7 ms.

Regional fractional area shortening was determined as follows. The LV and annular markers were used to divide the ventricle into 4 longitudinal (anterior, lateral, posterior, and septal) regions and 3 circumferential (basal, equatorial, and apical) levels (Figures 1 and 3). Fractional area shortening for each region was calculated as the ratio of end-diastolic area to end-systolic area.

Computation of LV Torsion

At each sample time, all marker Cartesian 3-dimensional coordinates (x, y, and z) were transformed into an internal cylindrical coordinate system (r, θ, and z) with origin at the centroid of the basal LV markers (6 to 9; Figure 1), z-axis passing through the centroid of the markers defining the apical transverse LV plane (2 to 5; Figure 1), and with 0° reference passing through the anterior LV basal marker (6; Figure 1). Positive angles were defined as counterclockwise as viewed from apex to base.

Epicardial marker m (2 to 5; Figure 1) for each apical level, b (b=b1, b2, b3; from ED_b to ED_{b+1}) during each beat, and torsional deformation φ_{mb}(t) at each sample time t (t=0@ED_b, 1, 2, . . . , T@ED_{b+1}) were computed as:

$$(1) \quad \phi_{mb}(t) = \theta_{mb}(t) - \theta_{mb}(T)$$

TABLE 1. Hemodynamics

	Non-CIMR		CIMR	
	Baseline	Chronic	Baseline	Chronic
MR (0-4+)	0.6±0.2	0.9±0.2	0.6±0.5	2.5±0.6*
LV dP/dt _{max} (mm Hg/s)	1921±440	1604±512*	1979±785	1256±506*
tau (τ, ms)	35±4	35±4	33±4	38±3*
LVEDP (mm Hg)	18±4	20±4	17±4	21±4*
EDVI (mL/m ²)	71±11	83±16*	64±18	90±20*†

MR indicates mitral regurgitation; LV dP/dt_{max}, maximum of first derivative of pressure vs time; tau, τ, time constant of diastolic pressure relaxation; LVEDP, LV pressure at end-diastole; EDVI, end-diastolic volume index.

*P<0.05 vs baseline.

†P<0.05 change from baseline in non-CIMR vs change from baseline in CIMR.

and mean LV torsional deformation [$\phi_m(t)$] for the 3-beat sequences comprising each run in each heart as:

$$(2) \quad \phi_m(t) = [\phi_{mb1}(t) + \phi_{mb2}(t) + \phi_{mb3}(t)]/3$$

Fractional ejection (FRAC) at each sample time (t) for each beat (b) was defined as follows:

$$(3) \quad \text{FRAC}_b(t) = [L\text{VV}_{\text{EDVb}} - L\text{VV}_b(t)] / (L\text{VV}_{\text{EDVb}} - L\text{VV}_{\text{EEb}})$$

where LVV_b(t) is LVV at time t, LVV_{EDVb} is LVV at EDV, and LVV_{EEb} is LVV at end-ejection for beat b. Mean fractional ejection at each sample time (t) [FRAC(t) for the 3-beat sequences comprising each run in each heart] was as follows:

$$(4) \quad \text{FRAC}(t) = [\text{FRAC}_1(t) + \text{FRAC}_2(t) + \text{FRAC}_3(t)]/3$$

For each LV free wall region (anterior, lateral, posterior), $\phi_m(t)$ was characterized by maximum LV torsional deformation (ϕ_{max}), and early diastolic torsional recoil ($\phi_{5\%}$) as the change in torsional deformation from end ejection to the first 5% of LV filling.

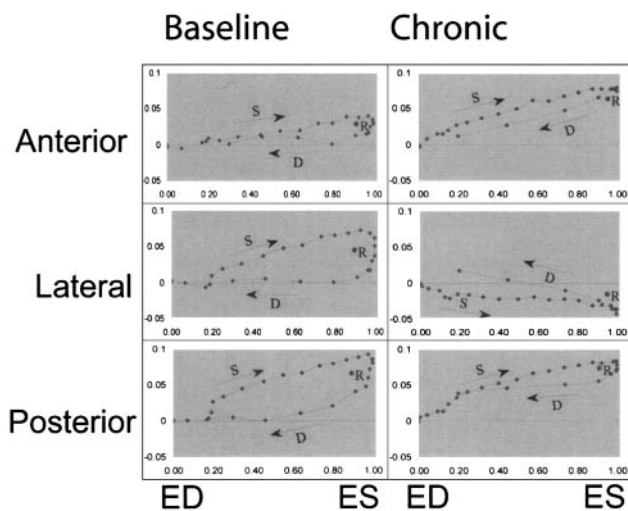


Figure 2. Regional (anterior, lateral, posterior) torsion (rad) versus fractional ejection (ED indicates end-diastole, 0% fractional ejection; ES, end-systole, 100% fractional ejection) before (baseline) and 7 weeks after (chronic) vessel occlusion in a representative animal in which CIMR developed. Arrows S and D indicate systole and diastole, respectively. Note that with CIMR, anterior torsion increased, whereas lateral and posterior torsion decreased. Early diastolic recoil (*R) decreased in all 3 regions after development of CIMR.

TABLE 2. Regional LV Torsion Dynamics

	Non-CIMR		CIMR	
	Baseline	Chronic	Baseline	Chronic
Anterior ϕ_{max} (°)	2.0±1.3	6.0±3.7*	3.3±4.9	4.9±3.7*
Anterior $\phi_{5\%}$ (°)	-1.2±1.0	-1.3±1.6	-1.4±1.1	-0.2±1.0*
Lateral ϕ_{max} (°)	3.8±3.3	0.6±0.6*	4.2±3.2	2.0±2.3*
Lateral $\phi_{5\%}$ (°)	-1.4±1.5	0.5±1.2*	-1.1±1.7	0.4±1.0*
Posterior ϕ_{max} (°)	4.4±2.5	2.8±2.0	6.1±4.3	3.9±1.9*
Posterior $\phi_{5\%}$ (°)	-2.8±2.1	-1.0±1.1*	-2.7±1.8	-0.7±1.9*

ϕ_{max} indicates maximum systolic torsion; $\phi_{5\%}$, torsional recoil during first 5% of diastolic filling.

*P<0.05 vs baseline.

Statistical Analysis

All data are reported as mean±1 SD. Changes in the CIMR and non-CIMR groups from baseline to chronic were analyzed using Student *t* test for paired comparisons. Changes from baseline to chronic conditions between the CIMR and non-CIMR groups were compared using a *t* test for unpaired comparisons.

Results

Table 1 summarizes hemodynamics at baseline and 7 weeks after inferior MI (chronic) in the non-CIMR and CIMR groups. Both CIMR and non-CIMR hearts exhibited reduced LV maximum dP/dt and increased end-diastolic volume index over the 7-week interval. The CIMR group exhibited increased time constant of diastolic pressure relaxation (τ) after infarction. Left-ventricular end-diastolic pressure also increased slightly in the CIMR.

Table 2 summarizes regional torsion dynamics at baseline and 7 weeks after inferior MI in the non-CIMR and CIMR groups. Seven weeks after inferior MI, both groups exhibited increased maximum systolic torsion (ϕ_{max}) in the anterior LV region and decreased systolic torsion in the lateral left ventricle. In the CIMR animals, systolic torsion was also decreased significantly in the posterior wall. Both CIMR and non-CIMR hearts had decreased early diastolic torsional recoil ($\phi_{5\%}$) in the lateral and posterior LV walls, but decreased recoil in the anterior LV was evident only in the CIMR animals. Figure 2 illustrates these torsion dynamics in one of the CIMR hearts in this study.

Table 3 summarizes end-diastolic septal-lateral and antero-posterior LV dimensions at the basal and apical levels. After inferior MI, non-CIMR animals had significant dilation of the

TABLE 3. End-Diastolic LV Basal and Apical Diameters

	Non-CIMR		CIMR	
	Baseline	Chronic	Baseline	Chronic
Basal S-L, cm	5.2±1.0	5.4±0.9	4.9±1.0	5.4±1.2*†
Basal A-P, cm	4.9±1.4	5.2±1.7*	4.9±1.2	5.5±0.10.4*
Apical S-L, cm	5.2±0.5	5.4±0.7	5.1±1.0	5.8±1.1*†
Apical A-P, cm	3.5±0.7	3.6±0.7	3.6±0.5	4.1±0.7*†

S-L indicates septal-lateral; A-P, anterior-posterior.

*P<0.05 vs baseline.

†P<0.05 change from baseline in non-CIMR vs change from baseline in CIMR.

NonCIMR				CIMR			
Anterior	Lateral	Posterior	Septal	Anterior	Lateral	Posterior	Septal
1.23±0.08	1.23±0.11	1.15±0.09	1.10±0.07	1.25±0.07	1.30±0.10	1.21±0.07	1.14±0.05
1.19±0.12	1.12±0.06	1.08±0.07	1.10±0.08	1.20±0.09	1.10±0.09	1.12±0.06	1.15±0.08
1.16±0.10	1.19±0.09	1.21±0.06	1.18±0.07	1.21±0.12	1.23±0.10	1.25±0.07	1.18±0.06
1.14±0.11	1.05±0.10	1.15±0.16	1.23±0.11	1.20±0.07	1.06±0.08	1.19±0.04	1.28±0.05
1.12±0.06	1.23±0.12	1.16±0.08	1.13±0.09	1.17±0.09	1.27±0.16	1.16±0.10	1.13±0.06
1.11±0.10	1.14±0.10	1.18±0.09	1.25±0.17	1.25±0.15	1.18±0.19	1.21±0.11	1.25±0.07

Figure 3. Regional fractional area shortening for non-CIMR (left table) and CIMR (right table) animals before (upper line in box) and 8 weeks after (lower line in box) MI. The marker array divided the LV into anterior, lateral, and septal regions longitudinally, and basal, equatorial, and apical regions circumferentially. Areas in which regional fractional area shortening was decreased 8 weeks after MI have a gray background; areas in which regional fractional area shortening was increased 8 weeks after MI are bold and italicized ($P < 0.05$, paired t test).

anterior-posterior diameter at the basal level, whereas CIMR hearts dilated in the septal-lateral and anterior posterior axes at both basal and apical levels. The change from baseline in the CIMR was also significantly greater than that of the non-CIMR in both axes at the apical level, and in the septal-lateral dimension at the basal level.

Figure 3 summarizes regional fractional area shortening for non-CIMR and CIMR animals before (upper line in box) and 8 weeks after (lower line in box) MI. In both CIMR and non-CIMR groups, fractional area shortening was reduced at the basal, equatorial, and apical levels for the lateral wall, and basal and equatorial levels for the posterior wall, approximately corresponding to the targeted area of the infarct. In both groups, fractional area shortening was increased at the equatorial and apical levels of the septal wall, but in the CIMR group only, fractional area shortening was increased at the apical level of the lateral and anterior walls.

Discussion

Both CIMR and non-CIMR animals had LV dilation and derangement in systolic torsion and diastolic recoil after inferior MI. The CIMR animals, moreover, exhibited significant reductions in posterior maximal torsion and anterior torsion recoil not evident in non-CIMR. These data, comparing regional torsion dynamics in CIMR with a postinfarct control group without CIMR, may provide important insights into the “ventricular disease” of CIMR.

Systolic Torsion

Systolic torsion, a wringing motion as the apex rotates with respect to the base about the LV long axis, minimizes transmural gradients of fiber strain and oxygen demand.^{8,9} Decreased systolic torsion, which should increase these gradients of fiber strain and oxygen consumption, has been reported in dilated cardiomyopathy⁴ and chronic (nonischemic) MR,⁵ possibly contributing to a cycle of progressive myocardial functional decline.

In a mathematical model studying the effects of torsion, normal torsion resulted in sarcomere shortening ranging from 0.20 μm at the epicardium to 0.48 μm at the endocardium. Removing torsion from the model, the epicardial sarcomeres shortened less (0.10 μm) and the endocardial sarcomeres shortened more (0.55 μm), thus increasing the transmural gradient of shortening.¹⁰ This corresponded to increased endocardial oxygen demand and a higher ratio of endocardial

to epicardial oxygen demand (1.08 versus 1.29).¹⁰ That study and others⁸ suggest that decreased torsion leads to a less efficient state in which the endocardium performs a greater share of the work of the ventricle. In the present study, inferior MI resulted in increased anterior wall torsion and decreased lateral wall torsion in both CIMR and non-CIMR animals. In the CIMR animals, torsion was also reduced in the posterior region after infarction. Decreased torsion in the lateral LV wall (and posterior wall in the case of the CIMR group) may result from contractile dysfunction in this region after the postero-lateral infarction (Figure 3). Decreased contractility causes less local force giving rise to torsion in that region. By the same token, the increased torsion in the anterior region may be related to compensatory hypercontraction in the septum and anterior LV wall in the CIMR. It may also result in part from a change in the material properties of the adjacent (lateral and posterior) myocardium after infarction that unloads the anterior region.

Reductions in systolic torsion, observed in the non-CIMR hearts in the lateral region and the CIMR hearts in both the posterior and lateral regions, would be expected to increase transmural gradients of fiber strain and oxygen demand in these regions, placing a relatively greater burden on the endocardial fibers. Even though the changes in torsion seen in this study are small, the deleterious effects may add up over the course of time and serve to compound the probably greater insults caused by increased wall stress in these already-compromised ventricles. Failure to modulate these mechanical and metabolic gradients may contribute to a vicious cycle of ventricular failure and functional decline observed in CIMR that persists even if the valve is repaired or replaced.

Specifically, decreased torsion, decreased contractile function, and LV dilatation may further compromise myocardial contraction and lead to progressive LV dilatation by increasing the burden on the already-dysfunctional (and relatively hypoperfused) endocardium.

Diastolic Recoil

Studies of normal hearts indicate that the bulk of torsional recoil occurs during isovolumic relaxation. Such recoil, which is linked to the rapid release of restoring forces in the extracellular matrix and to the relaxation and relengthening of contracted sarcomeres, is a likely determinant of myocardial

compliance during isovolumic relaxation and a contributor to diastolic LV suction, which may enhance filling.¹¹

The restoring forces contributing to diastolic suction may occur when end-systolic volume decreases below V_{eq} , the equilibrium volume of the ventricle, which is more likely to occur under increased inotropic states (which decrease ESV and increase V_{eq}). Restoring forces may also be released in response to the deformation of the 3-dimensional extracellular matrix and sarcomeric proteins such as titin.¹¹ Torsion has been considered an important deformation leading to such restoring forces. Similarly, the widespread perturbations in torsional recoil observed in this study suggest that loss of recoil may contribute to impaired diastolic LV suction in CIMR. This loss of recoil may be related to increased τ , as observed in this study. In a magnetic resonance imaging study of dogs, Dong et al showed that the rate of torsional recoil was an excellent predictor of LV relaxation through a variety of hemodynamic states and loading conditions.¹²

LV Dilation

LV dilation has been shown to be a powerful predictor of systolic function and survival in patients after MI.³ Although LV dilation in CIMR may exert many of its deleterious effects on ventricular performance through increased wall stress,¹³ the consequences of LV dilation, which were greater in the CIMR than the non-CIMR, on systolic torsion and recoil may also contribute to decreased ventricular function.

To see how increasing LV diameters might affect torsion, consider that the net moment giving rise to torsion can be modeled as the sum of opposing subendocardial and subepicardial vectors, each proportional to the length of its lever arm. Thus, although the angles of inclination of the subendocardial and subepicardial fibers are approximately equal (but opposite in sign), physiological torsion during systole is dominated by the subepicardial fibers because of their larger radii (and longer lever arms).¹⁴ Ventricular dilatation tends to increase the radii of both the subendocardial and subepicardial layers, thus allowing a relatively greater contribution from the subendocardium to the net torsion moment and decreasing maximum torsion. Taber et al predicted such a result by reasoning that in eccentric hypertrophy, the epicardial fibers would lose some of their mechanical advantage.⁸ Similarly, during early diastole, torsional recoil should be driven by the release of restoring forces in the extracellular matrix and myofibers of the subepicardium, which relax before those of the subendocardium. The relative equalization of the subendocardial and subepicardial lever arms again reduces the net torsional moment, decreasing early diastolic recoil, which may be important for LV filling at low pressures. Changes in the extracellular matrix after inferior MI mediated by matrix metalloproteinases¹⁵ may also affect the explosive release of restoring forces in early diastole.

Effect of Infarct Size

Despite our best efforts to induce infarctions of similar size and location,⁶ individual variations in coronary anatomy among the sheep contributed to different size infarctions that presumably affected outcome. Smaller infarctions resulted in lesser ventricular dilation without CIMR, larger infarctions

resulted in greater ventricular dilation associated with CIMR, and very large infarctions resulted in acute LV failure, arrhythmias, and death. The size of the infarct affected the amount of remaining contracting myocardium and thus may underlie the observed alterations in torsion. Using a similar ovine model of CIMR, Guy et al demonstrated that prophylactic ring annuloplasty (before infarction) could prevent IMR, but not secondary LV dilation. This again indicates that the size of the infarction, not the MR per se, may be the primary pathologic culprit responsible for adverse LV remodeling. The alterations in torsion observed in this study are dependent to some extent on infarct size in addition to degree of CIMR.

CIMR has been called a “ventricular disease” marked by continuing LV dilatation, worsening contractile function, and poor survival, whether the incompetent valve is replaced, repaired, or ignored.² After MI, LV dilation and contractile dysfunction lead to alterations in torsion and recoil that may result in increased gradients of oxygen demand and ventricular dysfunction. Thus, abnormalities in torsion may contribute to a persistent cycle of ventricular decline if such LV dilation is not addressed at the time of surgery. Although the changes in torsion may be more a function of infarct size rather than CIMR itself, these data suggest for the first time to our knowledge that alterations in torsion and recoil may play a part in the persistent systolic and diastolic dysfunction observed in CIMR. It remains to be seen whether procedures designed to remodel the LV (undersized annuloplasty,¹³ Acorn,¹⁶ or surgical ventricular restoration¹⁷) by decreasing LV radii of curvature or end-systolic volume will have a long-term effect on torsion or LV dysfunction in patients with CIMR.

Limitations

This study used a model of ovine chronic inferior infarction that differs from the clinical entity. The sheep have all undergone opening of the pericardium, cardiopulmonary bypass, and surgical manipulation of the mitral apparatus. Also, differences in ventricular and coronary anatomy between sheep and humans may influence the remodeling in chronic infarction and the distortions in systolic torsion and diastolic recoil. It is unknown whether reduction of CIMR would restore normal torsion dynamics. Studies are currently underway to investigate this hypothesis, but correction of torsion would probably require addressing both the LV dilation and the contractile dysfunction induced by the infarct.

Acknowledgments

The authors gratefully acknowledge the superb technical assistance provided by Carol W. Mead, Maggie Brophy, Katha Gazda, and Mark Grisedale.

References

1. Grigioni F, Enriquez-Sarano M, Zehr KJ, et al. Ischemic mitral regurgitation: long-term outcome and prognostic implications with quantitative Doppler assessment. *Circulation*. 2001;103:1759–1764.
2. Gorman RC, Gorman JH. Invited Commentary. *Ann Thorac Surg*. 2002; 74:1481.

3. Pfeffer MA, Pfeffer JM, Lamas GA. Development and prevention of congestive heart failure following myocardial infarction. *Circulation*. 1993;87:IV120–IV125.
4. Tibayan FA, Lai DT, Timek TA, et al. Alterations in left ventricular torsion in tachycardia-induced dilated cardiomyopathy. *J Thorac Cardiovasc Surg*. 2002;124:43–49.
5. Tibayan FA, Yun KL, Fann JI, et al. Torsion dynamics in the evolution from acute to chronic mitral regurgitation. *J Heart Valve Dis*. 2002;11:39–46.
6. Llaneras MR, Nance ML, Streicher JT, et al. Large animal model of ischemic mitral regurgitation. *Ann Thorac Surg*. 1994;57:432–439.
7. Tibayan FA, Rodriguez F, Zasio MK, et al. Geometric distortions of the mitral valvular-ventricular complex in chronic ischemic mitral regurgitation. *Circulation*. 2003;108:II116–II121.
8. Taber LA, Yang M, Podszus WW. Mechanics of ventricular torsion. *J Biomech*. 1996;29:745–752.
9. Arts T, Reneman RS, Veenstra PC. A model of the mechanics of the left ventricle. *Ann Biomed Eng*. 1979;7:299–318.
10. Beyar R, Sideman S. Left ventricular mechanics related to the local distribution of oxygen demand throughout the wall. *Circ Res*. 1986;58:664–677.
11. Bell SP, Nyland L, Tischler MD, et al. Alterations in the determinants of diastolic suction during pacing tachycardia. *Circ Res*. 2000;87:235–240.
12. Dong SJ, Hees PS, Siu CO, et al. MRI assessment of LV relaxation by untwisting rate: a new isovolumic phase measure of tau. *Am J Physiol Heart Circ Physiol*. 2001;281:H2002–H2009.
13. Bolling SF, Pagani FD, Deeb GM, et al. Intermediate-term outcome of mitral reconstruction in cardiomyopathy. *J Thorac Cardiovasc Surg*. 1998;115:381–386.
14. Ingels NB Jr, Hansen DE, Daughters GT, et al. Relation between longitudinal, circumferential, and oblique shortening and torsional deformation in the left ventricle of the transplanted human heart. *Circ Res*. 1989;64:915–927.
15. Mukherjee R, Brinsa TA, Dowdy KB et al. Myocardial infarct expansion and matrix metalloproteinase inhibition. *Circulation*. 2003;107:618–625.
16. Raman JS, Hata M, Storer M, et al. The mid-term results of ventricular containment (ACORN WRAP) for end-stage ischemic cardiomyopathy. *Ann Thorac Cardiovasc Surg*. 2001;7:278–281.
17. Athanasuleas CL, Stanley AW Jr, Buckberg GD, et al. Surgical anterior ventricular endocardial restoration (SAVER) in the dilated remodeled ventricle after anterior myocardial infarction. RESTORE group. Reconstructive Endoventricular Surgery, returning Torsion Original Radius Elliptical Shape to the LV. *J Am Coll Cardiol*. 2001;37:1199–1209.

Alterations in Left Ventricular Torsion and Diastolic Recoil After Myocardial Infarction With and Without Chronic Ischemic Mitral Regurgitation

Frederick A. Tibayan, Filiberto Rodriguez, Frank Langer, Mary K. Zasio, Lynn Bailey, David Liang, George T. Daughters, Neil B. Ingels, Jr and D. Craig Miller

Circulation. 2004;110:II-109-II-114

doi: 10.1161/01.CIR.0000138385.05471.41

Circulation is published by the American Heart Association, 7272 Greenville Avenue, Dallas, TX 75231

Copyright © 2004 American Heart Association, Inc. All rights reserved.

Print ISSN: 0009-7322. Online ISSN: 1524-4539

The online version of this article, along with updated information and services, is located on the
World Wide Web at:

http://circ.ahajournals.org/content/110/11_suppl_1/II-109

Permissions: Requests for permissions to reproduce figures, tables, or portions of articles originally published in *Circulation* can be obtained via RightsLink, a service of the Copyright Clearance Center, not the Editorial Office. Once the online version of the published article for which permission is being requested is located, click Request Permissions in the middle column of the Web page under Services. Further information about this process is available in the [Permissions and Rights Question and Answer](#) document.

Reprints: Information about reprints can be found online at:
<http://www.lww.com/reprints>

Subscriptions: Information about subscribing to *Circulation* is online at:
<http://circ.ahajournals.org/subscriptions/>